3rd International Conference on
PROTECTION OF HISTORICAL CONSTRUCTIONS
Lisbon, Portugal, 12 – 15 July, 2017

IN-PLANE BEHAVIOR OF RUBBLE STONE MASONRY WALLS: NUMERICAL AND ANALYTICAL APPROACH

Paulo B. Lourenço*, João M. Pereira*

* Institute for Sustainability and Innovation in Structural Engineering, University of Minho
e-mails: pbl@civil.uminho.pt, jpereira@civil.uminho.pt

Keywords: Rubble masonry; Shear capacity; Numerical analysis; Analytical models.

Abstract. *Unreinforced masonry construction is predominant in many urban areas world-wide. Many of these constructions are vulnerable to earthquakes, which are the main cause of damage and loss of cultural heritage. Understanding the in-plane behavior of masonry walls when subjected to horizontal loadings will improve the society capacity to preserve and protect this cultural heritage. An experimental campaign carried out at LNEC, Lisbon, allows calibrating non-linear numerical models used to study these elements in a more comprehensive way, performing parametric studies regarding the geometry, pre-compression level, boundary conditions and mechanical properties. The capacity to estimate the shear strength using available analytical models is also reviewed, applied and compared.*

1 INTRODUCTION

The increasing awareness for the preservation of the built heritage is a result of the social responsibility to protect its cultural identity, perpetuating it for future generations. Many of these constructions are vulnerable to earthquakes and its damage and collapse during a seismic event is a permanent threat to human lives. Considering past seismic events, it has been recognized that masonry buildings are vulnerable to these actions [1]. Masonry buildings are usually able to sustain the vertical loads [2], however, from the structural point of view; these buildings tend to fail to respond well to seismic loads [3]. The seismic behavior of a masonry building is defined by the interaction of the in-plane wall, the out-of-plane walls and the floor diaphragms through their connections. In general, the damage in masonry buildings can be essentially interpreted of two fundamental collapse mechanisms: out-of-plane and in-plane.

Several authors studied the behavior of masonry buildings when subjected to in-plane loading thorough experimental campaigns [4]. However, the high number of possible combinations of materials, geometry, boundary conditions, vertical loading, among others, makes the characterization of these elements a challenge. Numerical analysis can be considered auxiliary to experimental tests, allowing the assessment of masonry walls in-plane behavior when varying some parameters without the need of extensive experimental work.

This work studies the in-plane behavior of stone rubble masonry walls through a numerical campaign, being the models calibrated on the basis of an experimental campaign developed at LNEC, Lisbon. The calibrated models allow comprehensive parametric studies regarding the geometry, pre-compression level, boundary conditions and mechanical properties of the stone rubble masonry walls. This work also reviews, apply and compare different available analytical solutions to estimate the shear capacity of these elements.

2 NUMERICAL ANALYSIS

Numerical models were built to replicate the obtained experimental results. The Finite Element Method (FEM) was chosen to perform the simulations, using DIANA 9.4 software.

The experimental setup (Figure 1) was simulated including, besides the masonry wall, the steel support structure on the top of the wall ("B", Figure 1) and the steel anchors ("I", Figure 1) were simulated using springs (Figure 1d).

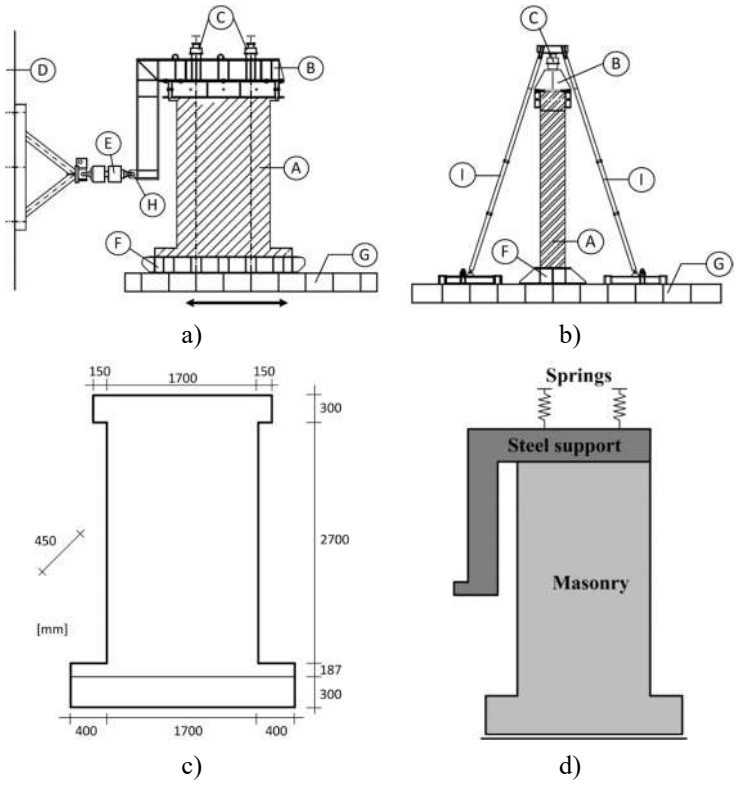

Figure 1: Experimental models: a) test setup at LNEC – front view; b) test setup at LNEC – lateral view; c) geometry of the models [dimensions in mm]; d) numerical model scheme. [(A) model; (B) "L" shaped top support; (C) vertical actuators; (D) reaction wall; (E) horizontal load cell; (F) bottom support; (G) seismic platform; (H) fixed horizontal translation; (I) steel anchors for applying the vertical load].

The masonry was modelled using a macromodelling approach, assuming the masonry as a composite material. This modelling strategy is an alternative to the micromodelling of the masonry components (units, mortar and interfaces) and assumes the use of average mechanical properties for masonry [5]. Another advantage of using this modelling strategy is the reduced computational time when compared with micro modelling, which usually required denser and complex finite element meshes [6]. This is particularly important in this presented work, as it is expected a large number of non-linear analysis for the parametric study and the analytical solutions study. In the specific case of rubble masonry, it is, usually, difficult to obtain detail information regarding the geometry and positioning of the units and the mortar thickness, which makes difficult the development of reliable micromodels. In our case, for each wall there are over 140 stones.

The FEM models used in this work were built using 2D plane stress elements. A regular mesh discretization was used using four-node quadrilateral isoparametric plane stress elements based on linear interpolation and Gauss integration – Q8MEM [7]. The springs were simulated using unidirectional single-point elements – SP1TR [7]. The final finite element mesh is composed of 3223 elements and 3403 nodes. For the steel structure, reference values were used for its linear mechanical properties, being 210 GPa for the Young's Modulus (E) and 0.2 for the Poisson coefficient (υ). The mechanical properties for masonry will be addressed during the model calibration process.

Similar to the experimental models, the horizontal force is registered as the horizontal reaction of the steel L-shaped structure on the top of the wall (corresponding to the "H" point of Figure 1). The horizontal displacement is measured in the exact same points used in the experimental models.

2.1 Model calibration

Because masonry exhibits non-linear behavior, a Total Strain Crack (TSC) model was selected. The Rotating Crack Model (RCM) was chosen for these models, as the experimental campaign showed predominant shear behavior [8]. Parabolic and exponential stress-strain relations were used to describe the tensile and compressive behavior respectively [7].

In order to use these constitutive models, it is necessary to define a set of parameters related to the mechanical properties of the material. Initially, some reference values for the mechanical properties of ancient masonry were used [5]. Later, the obtained results are compared with the experimental results and the initial input values are updated. This is a calibration process in which the objective is to approximate the numerical results with the experimental results. The steel behavior was kept elastic due to the considerable difference in stiffness when compared with the masonry. The equilibrium solution of the equations in each step of the non-linear analysis is obtained using a regular Newton-Raphson iterative method and a convergence criterion based on internal energy with a tolerance of 10^{-3}.

Different experimental models were tested and modelled, however in this work only the calibration of one of the models is presented. This model (Model 1) was built with a 1:4 ratio mortar and had an initial vertical load of 0.15 MPa. Table 1 shows the final mechanical properties after the calibration process. The obtained values for the different mechanical properties can be considered in the expected range. As an example, the Italian Standard [9] suggests values for the compressive strength of this kind of masonry up to 0.9 MPa which is quite close to the presented 1.03 MPa.

Table 1: Calibrated mechanical properties for Model 1 with 1:4 ratio mortar.

Property	Model 1
Young's Modulus, E (GPa)	1.750
Compressive strength, f_c (MPa)	1.030
Fracture energy in compression, G_c (N/mm)	9.000
Tensile strength, f_t (MPa)	0.060
Mode-I Fracture energy, G_f (N/mm)	0.250
Density, γ (kg/m3)	1900
Stiffness (springs), K (kN/m)	4.5E+06

The approximation of the numerical results with the experimental results can be seen in Figure 2a where both force-displacement curves can be compared. The obtained numerical curve shows a good agreement with the experimental curve. The shear resistance of the numerical model is 105.9 kN which corresponds to a difference lower than 1% when compared with the experimental results. This value was obtained at a 8.91 mm displacement which also corresponds to a difference lower than 1% when compared with the experimental results. Besides the force-displacement curves, also the damage pattern and the failure mode were compared. In the case of the numerical model the maximum principal strains were used as an indicator of the cracking. A comparison of the damage patterns of both experimental and numerical models can be seen in Figure 2b. From the numerical analysis, it is possible to see a shear failure with diagonal cracking, which is the same observation obtained for the experimental model.

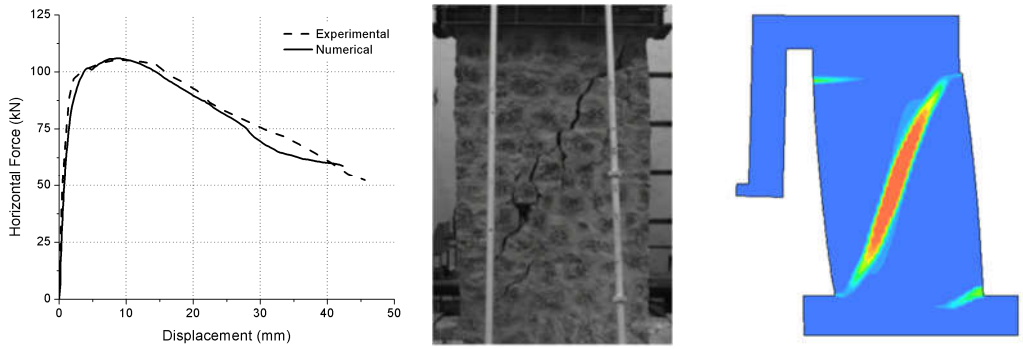

Figure 2: Comparison of the experimental and numerical results: a) force-displacement curve for Model 1; b) damage pattern for Model 1 (experimental and numerical).

2.2 Parametric studies

In order to clarify the influence and the interactions between different aspects of rubble stone masonry walls, a comprehensive parametric study was conducted using the calibrated numerical models already presented. The studied aspects were: a) geometry of the wall, focusing on the *h/l* relation; b) vertical load, as a function of the masonry's compressive strength; c) support conditions, adopting different stiffness supports at the top of the wall; and d) mechanical properties. Regarding the geometry, four *h/l* relations were studied ranging from 0.6 to 2.0. Three different vertical loads were applied ranging from 5% to 25% of the compressive strength of masonry. Different stiffness supports were introduced adding different height spandrels on top of the wall, these varied from 250 mm to 750 mm. The mechanical properties of Model 1 were changed ±25%. All of these parameters were combined and 108 new numerical models were developed.

It should be noted that in these new models the springs and the steel support structure on the top of the wall were removed, as the support conditions were changed and were in fact one of the parameters under the scope of this study. Instead, new elements (spandrel) were added to the model on top of the wall and its free edge had its rotations blocked. With these new conditions, these models are initially loaded with their self-weight and vertical load and later a horizontal loading is applied until failure. The same constitutive models and method for solving the non-linear equations are applied. The new numerical models were built with the same elements (Q8MEM) and the same mesh density.

New numerical models were built with different geometric configurations. The different *h/l* relations were obtained maintaining the same height of the wall and varying the length. Figure 3 shows the force-displacement curves for all considered geometries. It is possible to see that the geometry of the wall has a considerable influence on the maximum shear capacity. When changing the *h/l* relation from 0.6 to 1.0 it is possible to see a decrease in the maximum shear capacity of 55%. This decrease is the same when changing the *h/l* from 1.0 to 1.6. This reduction in the maximum shear capacity is less pronounced for higher *h/l* relations, being only 33% when changing from 1.6 to 2.0 (*h/l*), as can be seen in Figure 3d, where it is possible to compare the maximum shear capacities for different *h/l* relations for different vertical loadings. Besides the force-displacement curves, also the failure modes were analyzed. Keeping all other parameters unchanged, it was possible to see that for lower slenderness values the most common failure mechanism is through shear with diagonal cracking, whereas for higher slenderness values the failure mode tends to change for flexure mechanism with toe crushing and rocking.

Three different vertical loadings were considered as a function of the compressive strength of the masonry and varied from 5% to 25%. It is known that the pre-compression level influences the initial stiffness of the wall [4,10,11] however, in order to try to isolate the effect

of the pre-compression level, the initial stiffness of the walls was not changed when changing the vertical loading. This should be taken into account when analyzing these results. Figure 4 shows the force-displacement curves for all the considered pre-compression levels. As expected, the pre-compression level influences the response of these structural elements. When the vertical load decreases from 25% to 15% of the compressive strength, there is an average decrease of the maximum shear capacity of about 18%, whereas there is an average decrease of 33% of the maximum shear capacity when the vertical load decreases from 15% to 5% of the compressive strength. The failure mechanism where also analyzed, and in Figure 5 some examples are presented. It is possible to see that with the increase of the pre-compression level (vertical loading) the failure mechanisms tend to shift from flexural failure with toe crushing and rocking to shear failure with diagonal cracking.

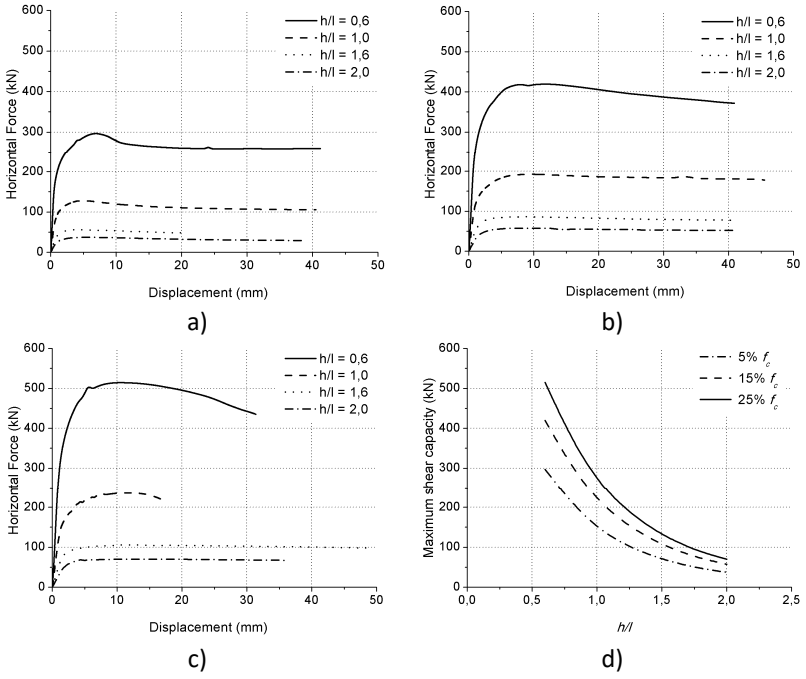

Figure 3: Influence of geometry for different vertical loading: a) 5% compressive strength; b) 15% compressive strength; c) 25% compressive strength; d) maximum shear capacity as a function of slenderness.

The stiffness of the support was changed by varying the height of a spandrel on top of the wall. The free edge of the spandrel has its rotations blocked by making sure that all nodes of the free edge of the spandrel have the same vertical displacement. Three different heights of spandrel were considered, being 250 mm, 500 mm and 750 mm. It was possible to see that the height of the spandrel on top of the wall has little influence in the maximum shear capacity of the wall. For higher pre-compression levels this influence is even smaller. Changing from 250 mm to 750 mm height with a 5% pre-compression level increases the maximum shear capacity an average of 8%, while with a 25% pre-compression level only increases the shear capacity an average of 2%. The failure mechanism is also not influenced by the changes in the support stiffness. Although the stiffness of the supports has little influence in the maximum shear capacity and the failure mechanism of these walls, it should be point out that this aspect (support conditions) has a substantially influence in the drift of these elements [11]. In this work, it is not possible to observe this phenomenon due to the material's mechanical properties. The mechanical properties for Model 1, namely the fracture energies, imply that both the numerical and experimental models do not have a pronounced softening after the peak, which doesn't allow for a proper drift analysis.

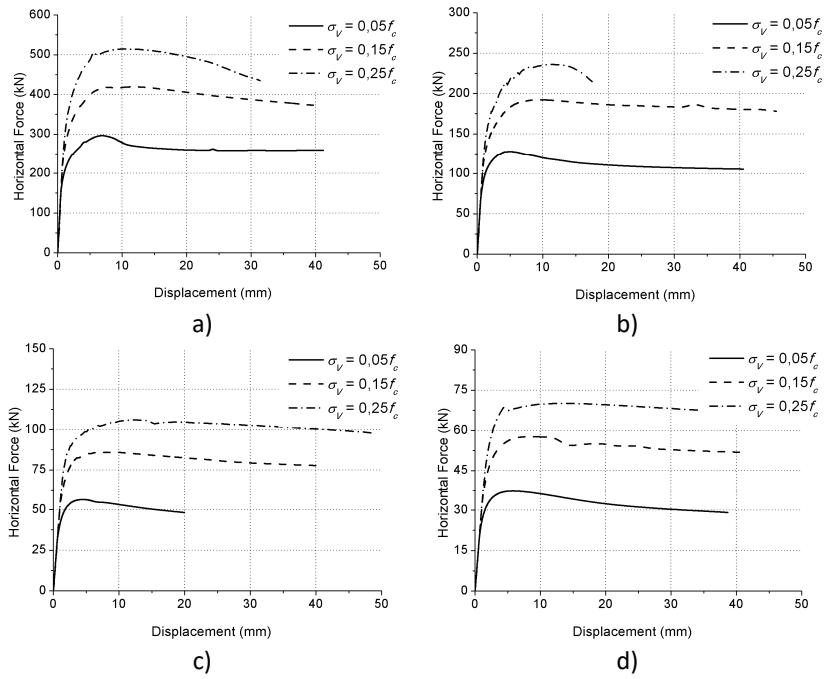

Figure 4: Influence of pre-compression level for different geometries: a) *h/l*=0.6; b) *h/l*=1.0; c) *h/l*=1.6; d) *h/l*=2.0.

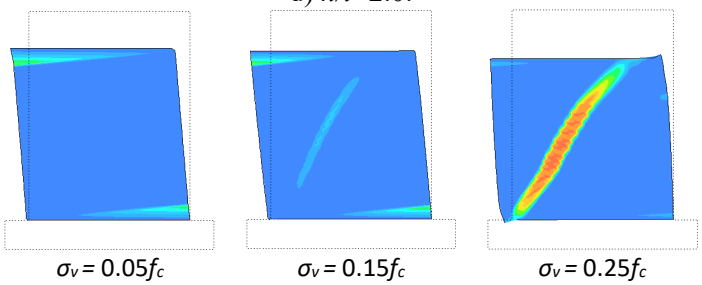

Figure 5: Examples of failure mechanisms for different pre-compression levels.

The mechanical properties from Model 1 were used as a reference and two additional sets of ±25% were created. It was possible to see that the mechanical properties influence the maximum shear capacity of these elements. A 25% reduction in the mechanical properties showed a reduction in the maximum shear capacity between 9% and 23% with an average of 14%, while an increase of 25% in the mechanical properties showed an increase in the maximum shear capacity between 6% and 15% with an average of 10%. Besides the force-displacement curves, also the failure mechanism was analyzed. It was possible to see that for lower mechanical properties the failure mechanisms tend to be governed by shear with diagonal cracking and for higher mechanical properties the failure mechanism tends to be governed by flexure with toe crushing and rocking.

3 ANALYTICAL STUDY

Several studies have been conducted with the objective of predicting the in-plane shear resistance of these structural elements through analytical solutions derived from experimental studies [12]. In this section the in-plane shear capacity of the above numerical models will be estimated accordingly to the existing documentation: a) Eurocode 6 – EC6 [13]; b) Italian Standard – NTC08 [9]; c) American Standard – FEMA [14]; and d) New Zealand Standard – NZSEE [15]. All these analytical methods consider the shear behavior of walls by equations to estimate the strength capacity of the walls according to the failure mode. The analytical

equations are discussed and the in-plane capacity is compared with the numerical results. The final analytical solutions from all the considered standards can be seen in Table 2.

3.1 Analytical equations

The in-plane resistance of walls, according to EC6 [13], is the minimum strength of the considered failure modes. It should be pointed that this standard doesn't prescribe for rubble masonry walls. Nonetheless this standard was also studied and applied in order to see if the prescribed analytical solutions can be applied also to rubble masonry walls. The lateral resistance of a wall where the failure is controlled through toe crushing is defined by the crushing of the compressed area in the bottom corner, not considering the tensile strength of masonry [16]. The stress distribution is commonly assumed as an equivalent rectangular stress block with a k coefficient equal to 0.85. With this stress equilibrium is possible to develop an equation able to estimate the lateral resistance of these elements with this failure mechanism [16] – Eq. 1. The European standard [13] only considers, in the case where shear mechanism are the dominant ones, the sliding of the bed-joint. This mechanism occurs when the acting shear stress in the effective section exceeds the shear resistance of the bed-joint. The shear resistance can be determined according to Mohr-Coulomb formulation [17] assuming the effective uncracked section length. The length of the effective compression zone is calculated neglecting the masonry tensile strength and assuming a simplified distribution of compression stresses [16,17]. The equation is easily deducted by these relations – Eq. 2. This standard presents reference values for the cohesion of masonry; however, it doesn't provide values for rubble masonry. The lower value presented by [13] was selected for these analysis, being a cohesion of 0.1 MPa.

$$V_F = \frac{M}{h_0} = \frac{N}{2h_0}\left(l - \frac{N}{0.85 f_c \cdot t}\right) \tag{1}$$

$$V_S = \frac{1.5l \cdot t \cdot f_{v0} + 0.4N}{1 + \frac{3h_0 \cdot t \cdot f_{v0}}{N}} \tag{2}$$

As the European standard, also the Italian standard [9] presents two analytical solutions to estimate the lateral resistance of wall, according to the failure mechanism. This standard provides prescriptions for rubble masonry and, it is in fact the only standard (of the selected) to contemplate this type of masonry. According to this standard, the lateral resistance of walls where the failure is controlled through flexural mechanism follows the same principals of EC6 [13] – Eq. 3. In the case where the failure is controlled through shear mechanism this standard is different from the EC6 [13]. The latter presented a solution to determine the lateral resistance for the sliding of the bed-joint, while the Italian standard [9] considers the diagonal tension as the only shear failure mechanism. This formulation assumes that the diagonal cracks are caused by the principal tensile stresses developing in the wall, with a critical value according to the tensile strength of masonry, and accounts for the influence of the geometric and load configuration. Assuming the masonry as an elastic, homogeneous and isotropic element, the lateral resistance of a wall failing in shear through diagonal cracking can be evaluated through Eq. 4.

$$V_F = \frac{M}{h_0} = \frac{N \cdot l}{2h_0}\left(1 - \frac{N}{0.85 f_c \cdot l \cdot t}\right) \tag{3}$$

$$V_D = l \cdot t \frac{1.5\tau_0}{b}\sqrt{1 + \frac{N}{1.5\tau_0 \cdot l \cdot t}} \qquad b = 1.0 \le {}^{h}\!/_{l} \le 1.5 \tag{4}$$

FEMA [14] presents four analytical solutions to determine the lateral resistance of walls, according to the four possible failure mechanisms. The lateral resistance of the wall is the minimum of the capacity calculated for each failure mechanism. For rocking mechanism, a rotation over the lower corner of the wall is assumed. This standard introduces a factor of 0.9 for the calculation of the lateral resistance over this failure mechanism – Eq. 5. For toe crushing (Eq. 6) and diagonal tension (Eq. 7) the analytical solutions presented by this standard are similar to the European equations, however some differences can be found. For toe crushing the vertical stresses distribution in the compressed area is considered 0.7fc instead of the 0.85fc in the European documents. In the case of sliding mechanism, this standard also follows the Mohr-Coulomb criteria; however, it doesn't take into account the moment which implies that the reduction in the effective length due to the horizontal cracking is not considered – Eq. 8. This standard presents some reference values for the cohesion of masonry, however, like the EC6 [13], it doesn't contemplate rubble masonry. From the suggested values, cohesion of 0.09 MPa was selected.

$$V_R = 0.9\alpha \cdot N \frac{l}{h} \tag{5}$$

$$V_C = \alpha \cdot N \frac{l}{h}\left(1 - \frac{N}{0.7 f_c \cdot l \cdot t}\right) \qquad \frac{l}{h} \geq 0.67 \tag{6}$$

$$V_S = \frac{0.75\left(0.75 f_{v0} + \frac{N}{l \cdot t}\right)}{1.5} \cdot l \cdot t \tag{7}$$

$$V_D = f_t \cdot l \cdot t \frac{l}{h}\sqrt{1 + \frac{N}{f_t \cdot l \cdot t}} \tag{8}$$

The NZSEE standard [15] presents one solution for walls failing under flexural mechanism with toe crushing and two solutions for walls failing under shear mechanism (sliding and diagonal tension). The analytical equation for toe crushing mechanism (Eq. 9) and sliding (Eq. 10) are similar to the European equations, already presented. The main difference of this standard consists in the differentiation of two possibilities when considering the mechanism of diagonal tension. Here, one solution is presented to account for the possibility of failure in the joints of masonry, following the Mohr-Coulomb principles (Eq. 11), and another solution is presented to account for the possibility of failure in the masonry units (Eq. 12). This document suggests some reference values for the cohesion, friction coefficient and the tensile strength of units. Because rubble masonry is not considered in this document, from the suggested values the following were selected: 0.1 MPa, 0.4 and 0.5 MPa for the cohesion, friction coefficient and tensile strength of units, respectively.

$$V_F = \frac{M}{h_0} = \frac{N}{h_0}\left(\frac{l}{2} - \frac{1}{2}\frac{N}{0.85 f_c \cdot t}\right) \tag{9}$$

$$V_S = \frac{1.5 f_{v0} \cdot l \cdot t + \mu N}{1 + \frac{3\frac{h_0}{l} f_{v0} \cdot l \cdot t}{N}} \tag{10}$$

$$V_D^j = \frac{f_{v0} \cdot l \cdot t + \mu N}{1 + \frac{h_0}{l}} \tag{11}$$

$$V_D^u = \frac{\sqrt{f_{ut} \cdot l \cdot t\left(f_{ut} \cdot l \cdot t + N\right)}}{2.3\left(1 + \frac{h_0}{l}\right)} \tag{12}$$

Where,

V_F – Flexural Strength	N – axial compressive force	α – coefficient for support conditions
V_R – Rocking Strength	h_0 – effective height	f_{v0} – cohesion
V_C – Toe Crushing Strength	l – length	τ_0 – average shear strength of masonry
V_S – Sliding Strength	t – thickness	μ – friction coefficient
V_D – Diagonal Tension Strength	f_c – compressive strength (masonry)	f_{ut} – tensile strength (units)
V_D^j – Diagonal Tension Strength, joints	f_t – tensile strength (masonry)	
V_D^u – Diagonal Tension Strength, units	b – coefficient for geometry	

3.5 Analytical results

All these normative documents were applied to the numerical models already presented and some examples can be seen in Table 3. The quality of the predictions was measured as the relation between the predicted value from the analytical solutions and the obtained numerical value as $V_{min,predicted}$ / V_{num}. Besides the lateral resistance of the wall, also the prediction of the failure mechanism was analyzed.

Table 3: Examples of analytical models applied to the numerical models.

Model	Numeric [kN]	Formulation	Prediction [kN]					$\frac{V_{min,predicted}}{V_{num}}$	Same failure mode?
			Flexure		Shear				
			Rocking	Toe Crushing	Sliding	Diagonal Cracking			
#8	53.60	EC6	42.52		42.94			0.79	yes
		NTC08	42.52		42.86			0.79	yes
		FEMA	43.27	44.30	64.09	46.69		0.81	yes
		NZSEE	42.52		42.94	59.28	100.57	0.79	yes
#16	170.38	EC6	169.60		160.49			0.94	yes
		NTC08	169.60		132.91			0.78	yes
		FEMA	220.12	153.53	163.30	127.91		0.75	yes
		NZSEE	169.60		160.49	178.62	222.92	0.66	no
#71	70.08	EC6	60.02		82.35			0.86	no
		NTC08	60.02		52.44			0.75	yes
		FEMA	82.37	71.39	112.02	44.72		0.64	yes
		NZSEE	60.02		82.35	66.98	83.59	0.86	no
#73	265.46	EC6	289.14		204.30			0.77	yes
		NTC08	289.14		171.43			0.65	yes
		FEMA	307.70	277.84	170.91	273.84		0.64	yes
		NZSEE	289.14		204.30	218.89	371.35	0.77	yes

The European standard [13] predictions ranged from 60% to 108%, with an average of 81%, relating to the numerical results. It should be noted that in only 3 cases (2.8%) the predictions from EC6 [13] gave higher strengths than the numerical values. This document was also able to correctly predict the failure mechanism in 70% of the models. In Figure 6a it is possible to see that there is a slight improvement in the results (in terms of coefficient of variation) for walls with higher slenderness ratios. Figure 6b shows the quality of the results according to the pre-compression level. It is possible to see that the scatter is similar in all the range of vertical loads under study; however, it is possible to see that for lower pre-compression levels the results seem to be closer to the numerical ones. In fact, for a 5%fc vertical load an average of 88% prediction was achieved, while for a 25%fc vertical load only an average 74% prediction was achieved.

The Italian standard [9] predictions ranged from 44% to 95%, with an average of 68%. This document was also able to correctly predict the failure mechanism in 55% of the models. The weakest results obtained with this standard were for the lower slenderness ratio wall (h/l = 0.6) with an average of 55%. The American standard [14] predictions ranged from 50% to 91%, with an average of 71%. This document was also able to correctly predict the failure mechanism

in 50% of the models. The New Zealand standard [15] predictions ranged from 56% to 98%, with an average of 77%. This document was also able to correctly predict the failure mechanism in 66% of the models. The behavior of these predictions according to the geometry of the wall and the pre-compression level is similar to the previous standards, lower coefficients of variation for slender walls and higher average predictions for lower pre-compression levels.

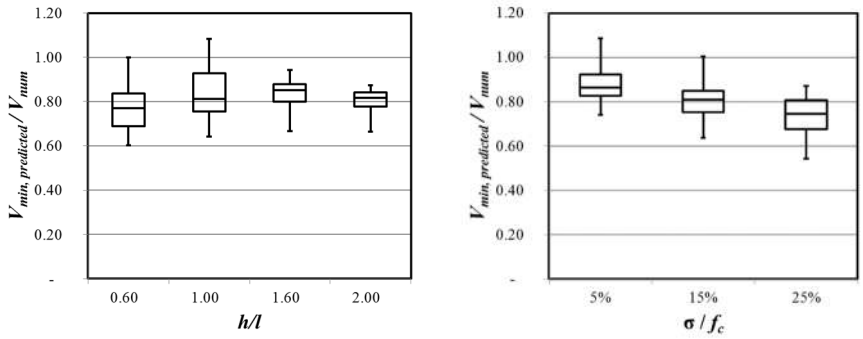

Figure 6: Analytical predictions using EC6 [13]: a) different geometries; b) different pre-compression levels (showing minimum, quartile 1, quartile 2, quartile 3 and maximum values).

Figure 7 shows a comparison of the average of predictions for all studied standards. It is possible to see that globally the EC6 [13] and the NZSEE [15] present the analytical solutions that better predicted the numerical results. These two standards were also the ones that had the higher number of correctly predicted failure mechanisms.

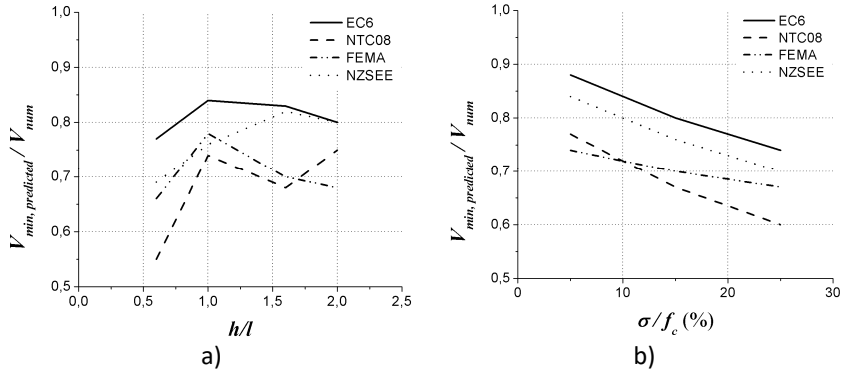

Figure 7: Comparison of the average predictions: a) different geometries; b) different pre-compression levels.

Because most of the available standards don't prescribe specifically for stone rubble masonry, selecting reference value for mechanical properties is not straightforward. One of the mechanical properties that had to be chosen from reference values was the masonry cohesion, being required for most of the available analytical solutions. Being so, the authors suggest that the cohesion could be related to the masonry tensile strength in the following equation:

$$f_{v0} = 2 f_t \tag{13}$$

Using the equation (Eq. 13) instead of the reference values and recalculating the analytical solutions presented earlier it is possible to see an improvement in the results. There is an overall increase in the predictions averages for all the studied standards, as can be seen in Figure 8, where a comparison between the averages of the predictions is presented for the EC6 (Figure 8a) and NZSEE (Figure 8b). It should be noted that there is an improvement, not only on the

average of the predictions, but also in the quality of the results, meaning that lower coefficients of variation were obtained (Figure 9).

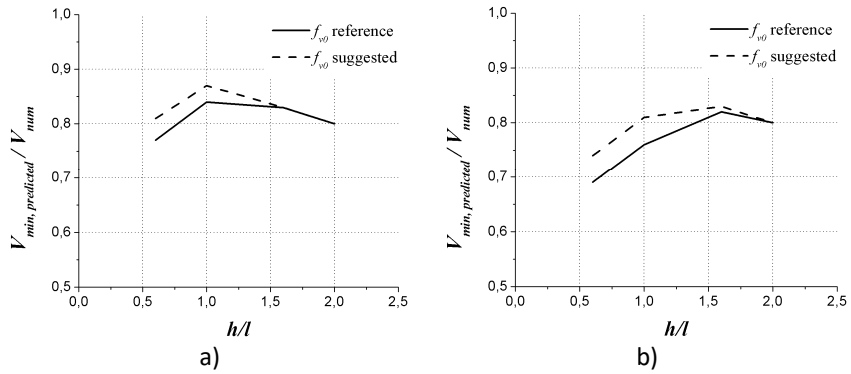

Figure 8: Examples of the influence of the suggested masonry cohesion: a) EC6 [13]; b) NZSEE [15].

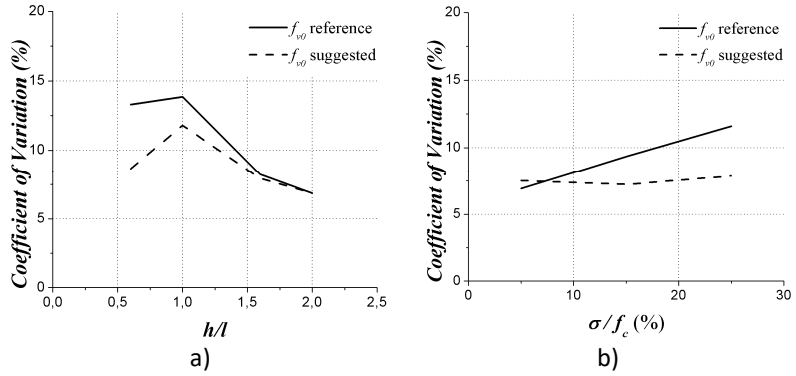

Figure 9: Examples of change in the coefficient of variation with the suggested cohesion: a) EC6 [13] for different geometries; b) NZSEE [15] for different pre-compression levels.

4 DISCUSSION AND CONCLUSIONS

The calibration of the numerical model (1:4 ratio mortars) is in agreement with the obtained experimental results. These numerical models seem capable of predicting the behavior of these elements when subjected to both vertical and lateral load. The maximum shear capacity is also well estimated and the evolution of the maximum principal strains are able to predict correctly the damage patterns of the experimental results. The calibrated mechanical properties for Model 1 (1:4 ratio mortar) are within the expected range for this kind of structural element.

In order to study the influence of different parameters in the response of these structural elements, an extensive parametric study was performed and presented. It was shown that the geometry and the pre-compression level acting on the wall are the parameters with the most influence in the shear behavior of these elements, both in terms of the maximum shear capacity and the failure mechanism. It was also possible to see that for this kind of walls the stiffness of the support doesn't influence the maximum shear capacity of these walls, however, it should be noted that this parameter has been reported [11] as having some influence in the post-peak behavior affecting the obtained drift. In this case, because of the obtained mechanical properties, it was not possible to verify this phenomenon. Varying the mechanical properties of these models also affects the shear behavior. A 25% variation in the mechanical properties leads to a variation between 6% and 23% of the maximum shear capacity of these structural elements.

Four different analytical solutions were studied, presented, applied and compared with the numerical and experimental results obtained before. It was possible to see that the analytical models, in general, achieved better predictions for lower pre-compression levels, and also for

slender wall, although less pronounced. It was observed that for these rubble stone masonry walls the EC6 [13] and the NZSEE [15] were the standards with the better predictions in terms of both the maximum shear capacity and the failure mechanism. Because most of the available standards don't take into consideration stone rubble masonry, a new equation for estimating the masonry cohesion was suggested. With the new cohesion introduced in the analytical models, the obtained results improved, not only in the average prediction, but also in lowering the coefficients of variation of the obtained results.

5 ACKNOWLEDGEMENTS

This work was performed under the research project: EpiCidade – Development of strengthening methods and experimental dynamic analysis of masonry buildings, with the reference QREN 13/SI/2011.

REFERENCES

[1] Lagomarsimo, S., "On the vulnerability assessment of monumental buildings". *Bulletin of Earthquake Engineering* 4, pp. 445-463, 2006.

[2] Betti, M., Vignoli, A., "Assessment of seismic resistance of a basilica-type church under earthquake loading: modelling and analysis". *Advances in Engineering Software* 39, pp. 258-283, (2008a).

[3] Corradi, M., Borri, A., Vignoli, A., "Strengthening techniques tested on masonry structures struck by the Umbria-Marche earthquake of 1997-1998". *Construction and Building Materials* 16, pp. 229-239, 2002.

[4] Elmenshawi, A., Sorour, M., Mufti, AA., "In-plane seismic behavior of historic stone masonry". *Canadian Journal of Civil Engineering* 37, pp. 465-476, 2010.

[5] Lourenço, PB., "Computational strategies for masonry structures". *Delft University of Technology*, 1996.

[6] Lourenço, PB., "Computations on historic masonry structures". *Progress in Structural Engineering and Materials* 4, pp. 301-319, 2002.

[7] TNO DIANA, "Displacement methods ANAlyser, release 9.4", *User's Manual*, 2009.

[8] Rots, JG., "Computational modelling of Concrete Fracture". *Delft University of Technology*, 1988.

[9] NTC08, "Technical regulations for the construction". *Italian ministry of the infrastructure*, 2008.

[10] Magenes, G., Calvi, GM., "Cyclic behaviour of brick masonry walls". *10th World Conference in Earthquake Engineering*, pp. 3517-3522, 1992.

[11] Petry, S., Beyer, K., "Influence of boundary conditions and size effect on the drift capacity of URM walls". *Engineering Structures* 65, pp. 76-88, 2014.

[12] Yi, T., "Experimental investigation and numerical simulation of an unreinforced masonry structure with flexible diaphragms". *Georgia Institute of Technology*, 2004.

[13] EC6-3, "Eurocode 6 – design of masonry structures – Part 3: simplified calculation methods for unreinforced masonry structures", 2005.

[14] FEMA 356, "Prestandard and commentary for the seismic rehabilitation of buildings". *Federal Emergency Management Agency*, 2000.

[15] NZSEE, "Assessment and improvement of the structural performance of buildings in earthquakes", 2006.

[16] Tomazevic, M., "Earthquake-resistant design of masonry buildings". *Imperial College Press*, 1999.

[17] Magenes, G., Calvi, GM., "In-plane seismic response of brick masonry walls". *Earthquake Engineering & Structural Dynamics* 26, pp. 1092-1112, 1997.